



# Wildfire Ash Composition and Engineering Behavior

Xenia Wirth, Ph.D., M.ASCE<sup>1</sup>; Vanessa Antunez, M.ASCE<sup>2</sup>; Dezire Enriquez<sup>3</sup>; Zuleyma Arevalo<sup>4</sup>; and Ramzieh Kanaan<sup>5</sup>

**Abstract:** After a wildfire event, ash is a newly formed surficial soil layer with microscale properties such as roughness, morphology, and chemical composition that may impact how ashes form fabrics in situ and so affect the overall hydrological conditions of a burned area (infiltration capacity, permeability, etc.). To examine the effects of ash microscale properties on macroscale behavior, eight wildfire ash samples from California were characterized physically (specific gravity, specific surface area, particle size, etc.), chemically (elemental composition, organic and inorganic carbon content, etc.), and geotechnically (strength, compaction, saturated hydraulic conductivity, etc.). The tested ashes were found to contain predominantly organic unburned carbons and carbonates derived from the combustion of calcium-oxalate rich fuels in temperatures likely ranging from 300°C to 500°C. Ashes had high specific surface areas because morphologically, particles had highly texturized and porous surfaces. Additional water was necessary to coat the particle surfaces, which led to high liquid limits and compaction optimum moisture contents. Hydraulic conductivity values were within range for silty sands (10<sup>-5</sup>–10<sup>-3</sup> cm/s), and specimens had friction angles near 30°. However, tested ashes consistently demonstrated high void ratios and low bulk densities during testing for strength, hydraulic conductivity, and compaction. These anomalies were attributed to unusual carbonate morphologies; the high interparticle friction of these phases allowed ashes to form looser fabrics than a typical silty sand and contributed to the measured high void ratios, low maximum dry unit weights, and high friction angles. Overall, we hypothesize that the relative amounts of inorganic versus organic constituents in our wildfire ash samples affected how the ashes formed fabrics and so affected their geotechnical properties. **DOI: 10.1061/JGGEFK. GTENG-11683.** © 2024 American Society of Civil Engineers.

Practical Applications: The role of wildfire ash in the postfire hydrological response of a catchment is not perfectly understood. Ash is a very heterogenous material whose properties are directly related to its formation environment (fuel type and accessibility, fire duration, and fire temperature, to name a few). This newly formed surface soil layer has unusual properties compared to natural soils, including low bulk densities and high porosities (sometimes up to 70% or more) in situ, but there is currently not enough information on ash properties in the literature to fully explain why. This study addresses this gap by providing physical, chemical, and geotechnical information about wildfire ashes. This is one of the first studies to specifically test wildfire ash maximum density, Atterberg limits, and shear strength. It provides geotechnical data to the community as well as information about ash chemical and physical properties. We hope that this study not only supplements the current literature on postwildfire landscapes but also informs researchers, engineers, and policy makers about how the formation environment of ash can influence its engineering behavior, such as strength, compressibility, and permeability.

# Introduction

The increased likelihood of wildfires in recent decades due to human-induced climate change and the associated hazardous impacts

Note. This manuscript was submitted on February 14, 2023; approved on January 31, 2024; published online on June 7, 2024. Discussion period open until November 7, 2024; separate discussions must be submitted for individual papers. This paper is part of the *Journal of Geotechnical and Geoenvironmental Engineering*, © ASCE, ISSN 1090-0241.

has spurred research into the hydrological response of postwildfire slopes. Many researchers in the geotechnical and geological communities have looked at the hydrological properties of postfire slopes at various temporal and spatial scales (Araújo Santos et al. 2020; Balfour and Woods 2013; Moody et al. 2009, 2013, 2016; Woods and Balfour 2010) and measured the effects of precipitation and other factors on the triggering of debris flows (Cannon et al. 2003; Cannon and Degraff 2015; Ebel et al. 2012; De Graff 2018; Larsen et al. 2009; Neary et al. 2003; Tiwari et al. 2020). The newly formed ash layer after a fire has been shown to impact the hydrological response. The spatial variability in the thickness of the ash layer leads to variability in surface runoff patterns on hillslopes (Bodí et al. 2014; Cerdà and Doerr 2008; Woods and Balfour 2010). Also, the physical and chemical composition of the ash and underlying soil layers (including hydrophobicity) can alter overland flow characteristics and in some cases may cause clogging of the underlying soil pores by fine ash particles (Balfour and Woods 2013; Certini 2005; Debano 1999; Doerr et al. 2000; Ebel et al. 2012; Onda et al. 2008; Woods and Balfour 2010).

Ash is unique from a geotechnical perspective because it lacks the geologic history associated with typical soil formation processes. It is formed and deposited within days to weeks, and its morphology, chemistry, and physical composition depend on the quality and composition of available fuels, combustion temperature, and combustion

<sup>&</sup>lt;sup>1</sup>Assistant Professor, Dept. of Civil and Environmental Engineering, CSU Fullerton, 800 N State College Blvd., Fullerton, CA 92831 (corresponding author). Email: xwirth@fullerton.edu

<sup>&</sup>lt;sup>2</sup>Civil Engineering Associate 1, LADWP, 111 N Hope St., Los Angeles, CA 90012.

<sup>&</sup>lt;sup>3</sup>Undergraduate Research Assistant, Dept. of Civil and Environmental Engineering, CSU Fullerton, 800 N State College Blvd., Fullerton, CA 92831; presently, Staff Engineer, Southern California Geotechnical, Inc., Yorba Linda, CA 92887.

<sup>&</sup>lt;sup>4</sup>Undergraduate Research Assistant, Dept. of Civil and Environmental Engineering, CSU Fullerton, 800 N State College Blvd., Fullerton, CA 92831; presently, Field Soils Technician, GeoTek Consultants Office, 1548 N Maple St., Corona, CA 92880.

<sup>&</sup>lt;sup>5</sup>Staff Engineer, Group Delta, 32 Mauchly STE B, Irvine, CA 92618; presently, Field Soils Technician, GeoTek Consultants Office, 1548 N Maple St., Corona, CA 92880.

duration (Keeley 2009; Úbeda et al. 2009; and references therein). Ash is a heterogeneous mixture of burned organic matter than can be presented as partially burned, organic-rich charcoal, inorganic mineral ash, and residual vegetation (Balfour and Woods 2013; Bodí et al. 2014; Moody et al. 2009; Woods and Balfour 2010). The relative proportions of organic char versus inorganic mineral ash are dependent on the conditions defined previously (Bodí et al. 2014; Pereira et al. 2013; Rodela et al. 2022; Úbeda et al. 2009). Rodela et al. (2022) suggested that that darker ashes with more organic compounds were combusted at low temperatures (< 350°C), and lighter-colored mineral ashes formed at mid to high temperatures (> 350°C). Others have shown that white-colored ash is predominantly CaCO<sub>3</sub> (Balfour and Woods 2013; Bodí et al. 2014; Úbeda et al. 2009) and that carbonate-rich ashes form in midrange combustion temperatures of 350°C-700°C (Balfour and Woods 2013; Bodí et al. 2014; Úbeda et al. 2009). Ash may be hydrophobic if the consumed vegetation contained naturally occurring hydrophobic compounds and the combustion conditions were favorable to transmit the volatized organic compounds onto the resultant ash (Bodí et al. 2011; Certini 2005; Debano 1999; Doerr et al. 2000).

Much work on wildfire ash has been focused on ash composition and hydrological behavior, but this material should also be analyzed from a geotechnical perspective. Particle microscale interactions (roughness, morphology, chemical precipitation, electrostatic bonding, etc.) influence macroscale geotechnical behavior (fabric formation, strength, hydraulic conductivity, etc.) (Lambe and Whitman 1969; Santamarina et al. 2001). Wildfire ash, as a newly formed surficial soil layer, has microscale properties that affect how ashes form fabrics in situ and so impact the overall hydrological conditions of a burned areas (infiltration capacity, permeability, etc.). Balfour and Woods (2013) observed the chemical, physical, and hydrologic properties of wildfire ashes and ashes generated in the laboratory at specific combustion temperatures. They noted that the carbonate particles in the ash had a significant effect on ash physical and hydrologic characteristics due to their morphology, electrostatic charges, and hydration reactions. Carbonate particles were hypothesized to aid in the absorption of water molecules and contribute to the unusually high bulk porosity of the wildfire ashes, as well as increased sorptivity and infiltration. Additionally, Rodela et al. (2022) noted that ashes combusted at higher temperatures (> 350°C) have higher electrical conductivity due to the presence of alkali and alkali earth metals, which leads to greater particle interactions.

Relationships observed by others between composition and macroscale behavior motivate us to more closely examine wildfire ashes as a geotechnical material. By exploring more deeply both the composition of wildfire ash and its geotechnical properties, we hope to provide insight into how microscale properties motivate macroscale behavior. We hypothesize that ash composition will influence how ashes form fabrics and so affect ash macroscale geotechnical properties such as strength and hydraulic conductivity; we will explore this by testing the physical (specific gravity, specific surface area, particle size, etc.), chemical (elemental composition, organic and inorganic carbon content, etc.), and geotechnical (strength, compaction, saturated hydraulic conductivity, etc.) properties of eight samples of wildfire ash from California.

# **Materials and Methods**

Eight samples of wildfire ashes were collected from the 2020 and 2021 fire seasons in southern California (Fig. 1). These samples were:

- Two samples from the Apple fire, August 2020, Cherry Valley, CA (33°59′25.3″N, 116°57′49.2″W) (A1 and A3).
- Two samples from the El Dorado fire, September 2020, Oak Glen, CA (34°03'29"N 116°59'22"W) (ED2 and ED3).
- Four samples from the French Fire, September 2021, Lake Isabella, CA (35°39′54.2″N 118°30′16.9″W) (FF1A, FF1B, FF2A, FF2B).

All three fires were located in the Mediterranean biome in southern California. The El Dorado fire, located in the Yucaipa Ridge of the San Bernardino Mountains, burned approximately 22,700 acres. The Apple fire burned 30,000 acres in Cherry Valley, CA. The French fire burned approximately 26,500 acres west of Lake Isabella in Kern County, CA. The dominant vegetative species in all three locations were southern California chaparral varieties, including chamise stands with manzanitas, ceanothus, and various sage scrub species (Parker et al. 2018).

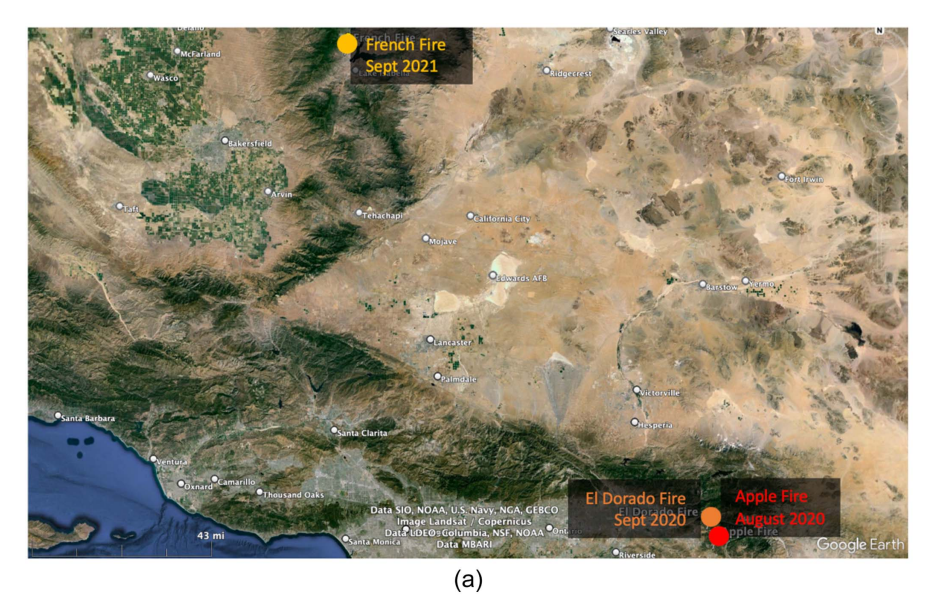




Fig. 1. (a) Sampling locations for the three fires used in this study; and (b) shaded rectangle highlights approximate region where all three fires were located in a satellite map of California. (Map data © 2024 Google; Data SIO, NOAA, U.S. Navy, NGA, GEBCO; Image Landsat/Copernicus; Data LDEO-Columbia, NSF, NOAA; Data MBARI.)

The California Nevada River Forecast Center daily precipitation maps were used to identify precipitation events that occurred between when the fires started and when sampling occurred. For the Apple and El Dorado fires, samples were collected before any significant postfire precipitation events. However, a precipitation event of 3.56 mm recorded rainfall was noted at a gauge station 3.6 mi from the location of the French Fire sampling, 13 days before sampling and 22 days after the fire began. Unfortunately, the site was still not fully contained at the time, so possible hydration of the fresh ash could not be avoided.

Various ash samples were collected in an effort to compare different types of materials that could be generated during combustion. Samples were then collected from surficial deposits of ash to a maximum depth of 5 cm below the ground surface. Care was taken to prevent the native soil from being included in the sampling. The composite ash of multiple samples taken from each site location was used for analysis.

# Physical Characteristics

Physical characterization tests included grain size distribution using sieve analysis for the complete ash samples and laser particle size analysis (PSA) for ash fractions passing the No. 100 sieve (0.15 mm) (Malvern Mastersizer). Specific gravity (SG) was tested using a gas 155 pycnometer (Quantachrome ULTRAPYC 1200e). Specific surface area testing was measured by the methylene blue dye drop procedure outlined in Santamarina et al. (2002). Munsell's color chart determined the sample hue, value, and chroma. For a more detailed analysis of ash properties, samples were also sieved into fractions based on particle size. Fractions included all particles retained on the No. 40 sieve (0.425–4 mm), retained between the No. 40 and No. 100 sieves (0.15–0.425 mm), retained between the No. 100 and No. 200 sieves (0.075–0.15 mm), and passing the No. 200 sieve (< 0.075 mm).

# Chemical Characteristics

Loss-on-ignition (LOI) testing (ASTM D7348), carbonate testing (G2121-i Picarro), and X-ray fluorescence (XRF) testing (Phillips PW 2400) measured the chemical composition of the wildfire ashes. The LOI testing was performed in two stages to isolate the combustion of unburned organic carbon from the decomposition of carbonates and other volatile mineral phases. First, the combustion of organic carbon phases occurred by heating the samples in a muffle furnace (Lindberg Blue M) to 500°C for 2 h. Then, the samples were cooled and weighed for total organic carbon (TOC) lost. The samples were placed back into the furnace and heated further to 950°C for 2 h. Cooled samples were weighed again, and the TOC and LOI were determined according to the following formulas [Eqs. (1) and (2)]. These temperatures were chosen based on Balfour and Woods (2013), where mass loss due to combustion of organic carbon was observed between 200 and 500°C

$$TOC = \frac{\text{mass loss after } 500^{\circ}\text{C}}{\text{initial mass}} \cdot 100 \tag{1}$$

$$LOI = \frac{\text{total mass loss after 950°C}}{\text{initial mass before igniting}} \cdot 100$$
 (2)

Total inorganic carbon (TIC) content was measured separately using a total carbon analyzer. Ash powders were sieved over the No. 40 sieve and ground to fine powder. The carbonate fractions of ash powders were dissolved in weak (10% v/v) phosphoric acid at room temperature overnight within individual evacuated Exetainer vials. An automate carbonate preparation device passed evolved  $CO_2$ 

into a G2121-i Picarro carbon isotope analyzer and carbonate contents and  $^{13}\text{C}/^{12}\text{C}$  ratios determined via cavity ringdown spectroscopy (CRDS). Carbon contents reported as total inorganic carbon (TIC by weight) [Eq. (3)]. Carbon isotope values were determined by comparison with international (NIST SRM 915B, IAEA NBS-18, Carrera Marble) and laboratory (CRCP90, CRC200) standards and reported in the typical  $\delta$ -notation( $\delta^{13}\text{C}$ ) [Eq. (4)] versus the VPDB standard in %. The isotope composition provided information about the origin of the carbon species in ash. TIC, projected calcium carbonate, and  $\delta^{13}\text{C}$  reproducibility are better than  $\pm 0.6\%$  by weight,  $\pm 4.4\%$  by weight, and  $\pm 0.3\%$ , respectively

$$TIC(\%) = \frac{\text{mass carbon}}{\text{initial mass}} \cdot 100 \tag{3}$$

$$\delta^{13}C(\text{permil}) = \left(\frac{\binom{13}{12}C}{\frac{13}{12}C}_{\text{sample}} - 1\right) \times 1,000\% \tag{4}$$

X-ray fluorescence testing was performed at Boral Resources (Taylorsville, GA) to measure the elemental composition of ashes. To remove organics and volatile materials from the sample, samples were ignited in a muffle furnace to 950°C for 2 h before infusing with a fusion matrix and testing. Then, the samples were exposed to X-rays, and the fluorescence allowed for the measurement of the relative percentage of the inorganic constituents (e.g., calcium, magnesium, iron, and silica).

The water drop penetration test (WDPT) method measured the hydrophobicity of the samples. One drop of distilled water (average volume = 0.023 mL) was placed on a smoothed ash sample surface in a 3.8-cm-diameter ring mold. Samples sieved over the No. 100 sieve were used to measure hydrophobicity, and data were taken in triplicate. The DeBano (1981) qualifications for the time required for a water droplet to penetrate the soil surface were used to classify soil water repellency: (<6 s: wettable; 6–60 s: slightly water repellent; 60–600 s: moderately water repellent).

# Geotechnical Properties

# **Atterberg Limits and Compaction**

Atterberg limit testing was performed on ash samples sieved over the No. 40 sieve [ASTM D4318 (ASTM 2010)] to identify the water contents at which ash transitioned from being powdery to liquidy. To identify the maximum possible density of wildfire ashes, a Harvard miniature compaction device was used to determine the optimum moisture content (OMC) and maximum dry unit weight (MDW). We hope this may inform future researchers about possible ranges of wildfire ash densities in the field. Samples were compacted in three layers (25 tamps per layer), and water content measurements were taken from the middle of each sample after extrusion. To identify error associated with operator variability, which has been discussed as a major flaw of using a Harvard miniature compaction device (Araújo Santos et al. 2019), control compaction tests using both the miniature device and the Standard Proctor were performed on a sample of silty sand native to the Fullerton area (sample contained 12.4% silt and 7.2% clay). The Harvard miniature device produced samples with a slightly higher MDW at lower OMC compared to the Standard Proctor (MDW $_{Harvard} = 16.6\%$  at OMC = 17.3% versus  $MDW_{SP} = 15.6 \text{ kN/m}^3 \text{ at OMC} = 18.2\%$ ). A similar result was observed by Araújo Santos et al. (2019). For wildfire ash samples prepared at water contents nearing the liquid limit, compaction by hand-tamping was necessary to prevent bearing capacity plunging failure.

#### **Hydraulic Properties**

The saturated hydraulic conductivity testing of wildfire ash mixtures was performed in a rigid wall permeameter (D = 11.4 cm) under constant head [ASTM D2434 (ASTM 2000)] to determine their water flow characteristics. Samples were prepared by placing a thick layer of wildfire ash (4-6 cm) above a layer of compacted Silver #20 sand (10 cm). This was done to both conserve the quantity of ash for other testing and to simulate a field scenario where ashes are deposited above native soils following a wildfire event. The compacted sand had a unit weight of 15.8 kN/m<sup>3</sup>, and the wildfire ash layers were prepared in both a loose state (target 50% relative compaction) and a dense state (target 85% relative compaction). Prepared specimens were saturated for a 24-h period and then tested for saturated hydraulic conductivity at hydraulic gradients of 3-4 (depending on the final height of the specimen after saturating). Void ratios were calculated from weight/volume relationships using the dry weight of ash used  $(W_s)$ , the diameter of the permeameter (D), the height of the ash layer after saturation  $(H_{\text{saturated}})$ , the unit weight of water  $(\gamma_w)$ , and the measured SG values [Eq. (5)]

$$\gamma_d = \frac{W_s}{\frac{\pi D^2}{4} \cdot H_{\text{saturated}}}; \qquad e = \frac{SG \cdot \gamma_w}{\gamma_d} - 1$$
(5)

The equivalent hydraulic conductivity method was used to estimate the saturated hydraulic conductivity of the ash layer, assuming that vertical flow dominated [Eq. (6)] (Budhu 2011)

$$k_{\text{eq}} = \frac{H_0}{\frac{h_{\text{ash}}}{k_{\text{ash}}} + \frac{h_{\text{sand}}}{k_{\text{sand}}}} \tag{6}$$

where h = thicknesses of the respective layers (measured after saturation, before beginning the conductivity test). The equivalent hydraulic conductivity of the system and Silver #20 sand were measured directly.

Sorptivity was measured using a mini disk infiltrometer (Meter Group) as an indication of how readily the ashes absorbed water. Dry samples were prepared as loosely as possible using dry pluviation into a consolidometer mold (height = 2.54 cm, diameter = 6.35 cm) and then compressed in a pneumatic consolidation load frame (Gilson HM series) to stresses of 1, 25, and 50 kPa. The stresses were applied by the consolidometer to simulate the application of 0.2–10 ft of overburden to the lightweight ash layer. The samples compressed at 1 kPa were prepared intentionally to simulate ash that had been freshly deposited after a wildfire. The suction rate for the mini disk infiltrometer was set at 2 cm<sup>-1</sup>. Sample A3 was not measured because there was an insufficient quantity of ash to run the analysis.

Sorptivity was calculated based on the steady-state infiltration rate measured during testing, after Zhang (1997) [Eq. (7)]. Cumulative infiltration (in cm) was plotted against the square root of time, and the curve was fitted with the function

$$I = C_1 \sqrt{t} + C_2 t \tag{7}$$

where  $C_1$  and  $C_2$  = fitting parameters;  $C_1$  (cm/s<sup>1/2</sup>) = measure of the soil sorptivity; and  $C_2$  (cm/s) = related to hydraulic conductivity.

# Strength

Analysis of the ash friction envelope was done using both a direct shear (ELE 26-2114) and a ring shear device (GDS RSA). The direct shear device was used to measure the shear strength of wildfire ash deposited as a thin layer (1 cm thick) above a compacted layer of commercially available sand (Silver #20, USCS classification

SP, particle size range 0.425–0.85 mm). The setup was designed such that the shearing plane always manifested at the center of the ash layer. A loosely deposited layer of ash (1 cm thick) above a densely compacted sand layer (1 cm thick) simulated a depositional environment just following a wildfire event. Tests were run in both the dry and saturated conditions at normal stresses of 25, 50, 100, and 200 kPa.

The ring shear device was used to determine the friction envelope of just the finer-grained portion of the wildfire ash (sieved over the No. 100 sieve) in a drained, saturated condition. The ring shear device measured a drained, residual strength of thin (5 mm thick) specimens and was used to try to estimate the minimum strength of wildfire ashes. Tests were run at a displacement rate of 0.01 mm/min to minimize shear-induced pore water pressures. Tests were run at both very low normal stresses (5–40 kPa) and at moderate normal stresses (50, 100, and 200 kPa) to capture variations in friction angle with normal stress. For both shearing methods, single stage tests were run, and new specimens were prepared for each value of normal stress.

# **Results and Discussion**

# Physical Characteristics

The wildfire ashes were a combination of very fine, powdery mineral ash particles, larger, charred organic fragments (char), and residual underlying native soil and vegetation. Colors of specimens ranged from a whitish tan to black (Table 1). The USCS classifications for the wildfire ashes ranged from SP-SM to SM. The silt fraction ranged from 5.6% to 28% (Fig. 2), and less than 0.2% of the ash samples were considered clay-sized particles. Only one sample (FF1A) had a physical texture that was similar to a natural silty sand because it was a mixture of burned sand and ash. The other samples felt powdery and "fluffy" instead. The black-colored ashes (A1, FF1A) were the only ashes to have fines contents less than 10%, which agrees with observations by Rodela et al. (2022) that increasing combustion temperatures produces lighter colored ashes with finer particle sizes.

Specific gravity values for wildfire ash samples ranged from 2.45 to 2.75 with an average value of 2.65 (SD = 0.096) (Table 1). Whereas most of the samples had SG values within the range expected for natural soils (2.6–2.8), samples A3 and FF1B were lower (2.45 and 2.59, respectively) due to unburned char particles in the ashes. A3 and FF1B had the highest organic carbon content (discussed subsequently), and char particles are lightweight, which would reduce the overall SG (Rodela et al. 2022). The specific surface area ( $S_s$ ) of the wildfire ashes ranged from 1.83 to 4.89 m²/g (Table 1). These values were high compared to typical  $S_s$  values for sand (1–40 × 10<sup>-3</sup> m²/g) and silt (0.04–1.1 m²/g) (Santamarina et al. 2001).

The higher  $S_s$  values were attributed to the ash constituents. Scanning electron microscope (TM 1000) images demonstrated complex morphologies such as particles with highly texturized, flaky surfaces; spongy particles reminiscent of the plant structure; stacked, sheeted structures; and prismatic crystals (Fig. 3). The organic char phase had spongelike morphologies with extensive internal pore networks that increased the overall surface area [Fig. 3(d)]. These were similar in appearance to unburned carbon found in fly ashes (Wirth et al. 2019; Yeboah et al. 2014) and were larger, angular particles (Rodela et al. 2022) that were crushable with finger pressure (observed in the laboratory). Additionally, the flaky morphologies with complex external surface features were likely fused masses of nanocrystalline calcitic grains formed from

Table 1. Physical characteristics of wildfire ashes

Sample	% passing No. 100	% fine-grained	% clay (< 2 $\mu$ m)	USCS	SSA $(m^2/g)$	SG	Color
FF1A	13.92	7.26	0.05	SW-SM	3.67	2.73	7.5 YR 2/1
FF1B	32.03	24.05	0.04	SM	1.83	2.59	7.5 YR 6/2
FF2A	33.09	23.24	0.06	SM	2.45	2.65	7.5 YR 6/2
FF2B	31.97	22.66	0.10	SM	3.06	2.65	7.5 YR 6/2
ED2	50.00	26.56	0.06	SM	4.28	2.75	7.5 YR 5/2
ED3	18.71	12.01	0.06	SP-SM	4.89	2.73	7.5 YR 6/2
A1	34.27	26.34	0.11	SM	2.45	2.73	7.5 YR 9/2
A3	8.49	5.80	0.02	SW-SM	4.89	2.45	7.5 YR 1/1

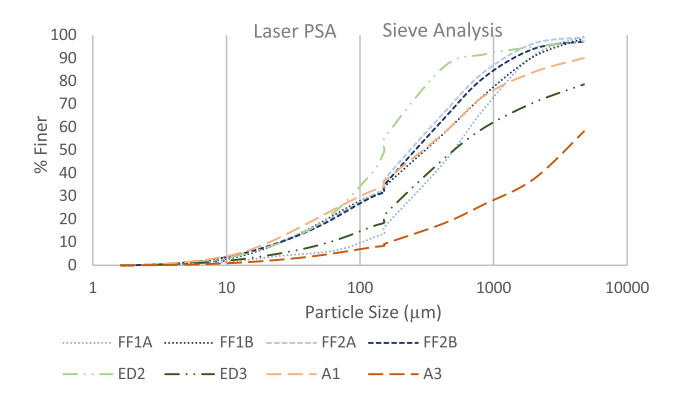


**Fig. 2.** Particle size analysis of ash using laser PSA (< 150  $\mu$ m) and sieve analysis (> 150  $\mu$ m). The slight misalignment between measurement methods at 150  $\mu$ m was due to one method using a wet dispersion technique and the other a dry vibration method.

the thermal decomposition of calcium oxalate at temperatures between 450°C and 500°C (Shahack-Gross and Ayalon 2013). Shahack-Gross and Ayalon (2013) studied the decomposition of calcium oxalate to calcium carbonate during laboratory combustion of wood branches at 500°C and 900°C and found similar morphologies to those shown in Fig. 3. Balfour and Woods (2013) also observed similar morphologies in lab-generated wildfire ashes burned at 500°C and identified them as carbonates [Figs. 3(a, b, and e)]. Chemical characterization (discussed subsequently) confirmed the presence of carbonates in our wildfire ashes.

### Chemical Characteristics

The inorganic elemental composition of wildfire ashes can be divided, after the manner of Vassilev et al. (2013), into forming (> 10%), major (1%–10%), minor (0.1%–1%), and accessory elements (< 0.1%), based on their relative XRF percentages (2013). Forming elements included Si, Ca, and Al; major elemental

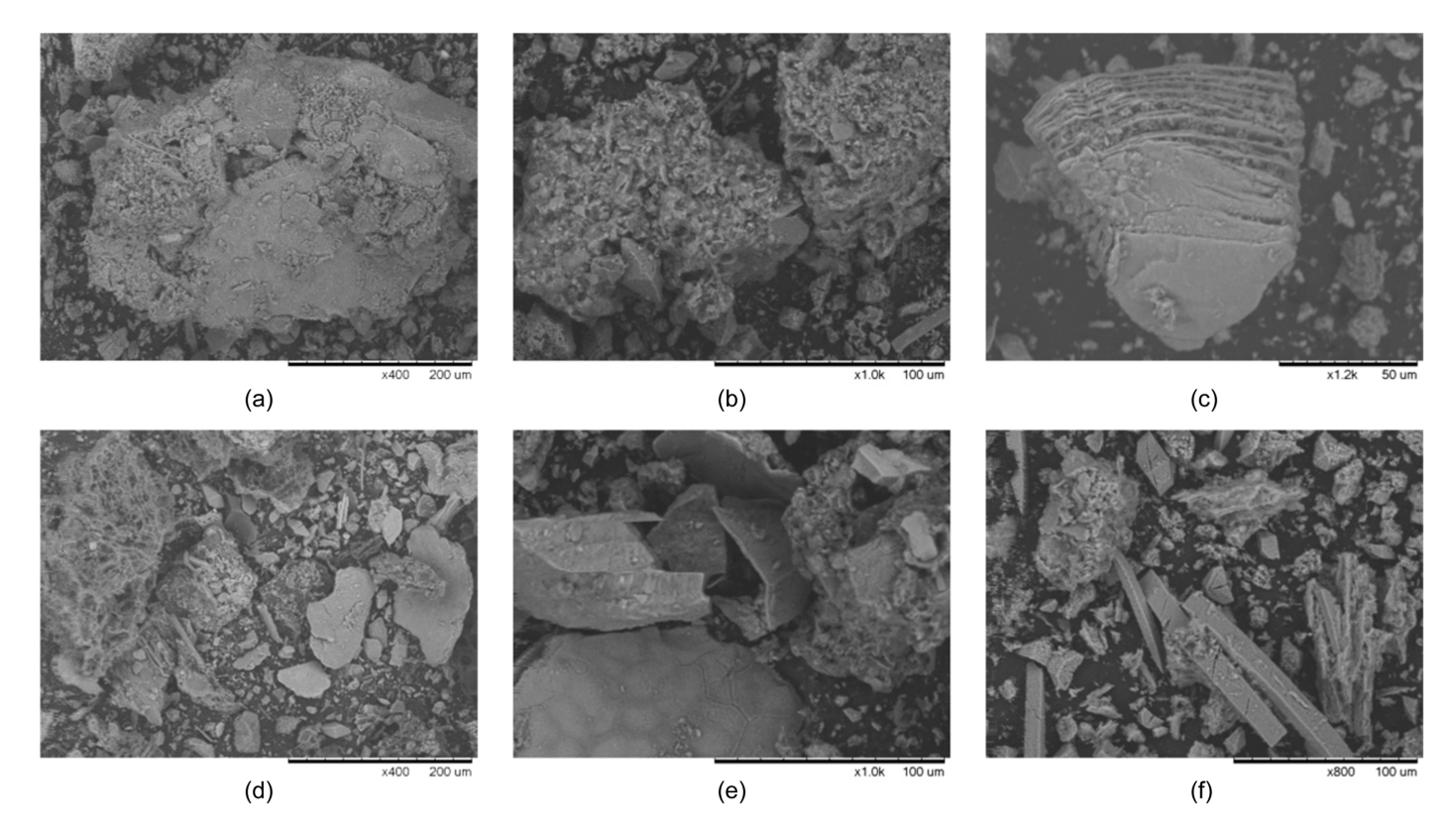


**Fig. 3.** SEM TM 1000 images of wildfire ashes showing (a, b, and e) flaky, texturized surfaces; (c and f) sheeted and prismatic structures; and (d) char (a–c correspond to A1, FF2A, and ED3; and d–f correspond to A3, FF1A, and FF1B).

Table 2. Inorganic elemental composition of wildfire ashes, expressed as oxide percentages

Sample	$SiO_2$	$Al_2O_3$	$Fe_2O_3$	$SO_3$	CaO	Na <sub>2</sub> O	MgO	$K_2O$	$P_2O_5$	$TiO_2$
FF1A	42.3	10.7	2.37	0.33	26.4	2.29	2.54	3.43	0.74	0.30
FF1B	66.7	16.1	2.9	0.21	5.25	3.68	0.79	2.88	0.31	0.44
FF2A	57.7	12.4	2.55	0.31	15.2	2.42	1.24	2.73	0.87	0.45
FF2B	55.6	12.7	2.79	0.56	14.4	2.59	1.70	4.72	1.44	0.41
ED2	40.2	17.2	8.59	1.62	19.0	1.11	3.05	4.87	1.92	1.15
ED3	30.2	12.7	8.43	1.01	26.3	0.99	4.28	9.26	4.12	0.93
A1	9.53	5.23	4.87	1.04	51.7	0.30	6.02	12.9	2.21	0.59
A3	48.7	15.5	8.39	0.71	15.9	1.62	3.21	3.83	1.13	1.05

quantities included Fe, Na, Mg, and K; and minor elements included Ti, S, and P (Table 2). Typically, wildfire ashes were most enriched in silicon (> 30% by weight across all ashes except A1). Calcium content varied the most between samples, ranging from 5% to 52% by weight.

Our findings are consistent with elemental compositions reported by others. Atomic compositions of calcium and silicon were both high in gray ashes sampled by Rodela et al. (2022) (Ca = 10.7%, Si = 8.6%, O = 80.4%, and Al = 2.7%). In a study by Balfour and Woods (2013), laboratory ashes combusted between 500°C and 700°C were enriched in calcium over other elements (Ca = 13.35%, K = 5.56%, Al = 1.02%, and Mg = 3.22%). Additionally, Sánchez-García et al. (2023), references within a review by Bodí et al. (2014) and Pereira et al. (2012) all showed ashes contained more extractable calcium than the other alkali and alkaliearth metals. Other studies often report chemical composition based on aqueous analysis of extractable elements, so the results will not be directly comparable to those displayed here, but trends in elemental composition were similar.

The fine, inorganic mineral ash contained carbonates, based on the foaming reaction when ashes were exposed to acid and the total inorganic carbon analysis (Table 3). The most carbonate-rich ashes were FF2A (TIC = 2.42%), A1 (4.56%), and FF1B (4.84%). The isotope compositions of the carbon ranged from approximately -22 to -25permil, which is within the range of plant biomass that exhibit C3 photosynthesis (-20 to -37 permil) (Kohn 2010). The isotope analysis indicated that the carbonates originated from plant biomass, likely the thermal decomposition of calcium oxalate from fuels during the fire event (Bodí et al. 2014; Monje and Baran 2002; Shahack-Gross and Ayalon 2013).

The loss-on-ignition of wildfire ashes fluctuated between fire sites and between samples taken at the same site (Table 3). LOI values ranged from 3.5% to 22%. Some samples were organic rich (A3, FF1A); their TOC/LOI ratio was very high (0.88 and 0.76, respectively), and most mass loss occurred in the 20°C–500°C range. In contrast, some samples (A1, FF2A, FF2B) had low organic content and more mass loss in the inorganic range (500°C–950°C). Fractioning the ashes showed that organic content was not

Table 3. Carbon content of wildfire ashes

Sample	TOC (%)	LOI (%)	TOC/LOI	TIC (%)	$\delta^{13}$ C (permil)
FF1A	2.69	3.52	0.76	0.18	a
FF1B	7.55	15.9	0.48	4.84	-22.1
FF2A	2.31	7.50	0.31	2.42	-23.0
FF2B	2.13	5.64	0.38	1.52	-22.4
ED2	2.93	6.14	0.48	0.86	-22.2
ED3	3.45	6.92	0.50	1.23	-25.3
A1	2.27	15.0	0.15	4.56	-22.1
A3	18.9	21.4	0.88	1.10	-22.8

<sup>&</sup>lt;sup>a</sup>Sample could not be tested for carbonate isotopes.

concentrated in any particular size fraction of the wildfire ashes [Fig. 4(a)]. Inorganic mineral phases, however, were concentrated in the smaller particle sizes [Fig. 4(b)].

Organic content was loosely associated with color (Table 1) because the darkest ashes tended to contain the highest amount of organic carbon (Bodí et al. 2011). However, color was not a good predictor of TOC content in general because the varying shades of gray in the samples were not well correlated with specific percentages of mass lost during combustion. This has been observed by others (Balfour and Woods 2013; Bodí et al. 2011, 2014; Pereira et al. 2013).

The presence of both carbonate and organic carbon phases in the wildfire ashes, combined with an isotope composition within the range of plant biomass and morphological similarities between these ashes and those created in the laboratory at combustion temperatures of 500°C (Balfour and Woods 2013; Shahack-Gross and Ayalon 2013), would indicate that the combustion temperatures at each fire site likely varied between 300°C and 500°C. Temperatures were high enough to partially combust a carbon-rich and calcium oxalate-containing fuel source into an ash that contained both carbonates and organic carbon phases (Balfour and Woods 2013; Bodí et al. 2014; Rodela et al. 2022; Shahack-Gross and Ayalon 2013; Úbeda et al. 2009). Only one sample (A1) was likely to have been combusted at temperatures near or slightly beyond 500°C, given that it had the lowest TOC/LOI ratio (0.15), a higher carbonate content (TIC = 4.5%), and a whitish color (Balfour and Woods 2013; Rodela et al. 2022; Úbeda et al. 2009).

Hydrophobicity was observed in wildfire ash samples FF1A, A3, and ED3. FF1A and ED3 were slightly water repellent (t = 9.1 s and 13.9 s, respectively), and A3 was moderately water repellent (t = 512.0 s). Although A3 had the highest TOC content of all samples, FF1A and ED3 did not have the next highest TOC contents, indicating that organic carbon content was not a satisfactory predictor of hydrophobic behavior. Doerr et al. (2000) and references therein proposed that a slight to moderate repellency in soils is due to the inclusion of some hydrophobic particles in the overall soil matrix rather than the coating of all particles in hydrophobic compounds, and we believe this to be true for the tested wildfire ashes.

# Geotechnical Properties

# **Atterberg Limits**

The liquid limit for wildfire ashes ranged from 28.4% to 82.1%, and the average liquid limit was 45.1% (Table 4). Samples A1 and A3 were the only two to have liquid limits above 50%. Generally, samples prepared at water contents up to approximately 25% felt dry, loose, and powdery to the touch, with a "fluffy" texture. In the extreme case of A3, the sample retained a loose, powdery structure up to a water content of approximately 70%. The plastic limit thread test indicated that samples were nonplastic because samples

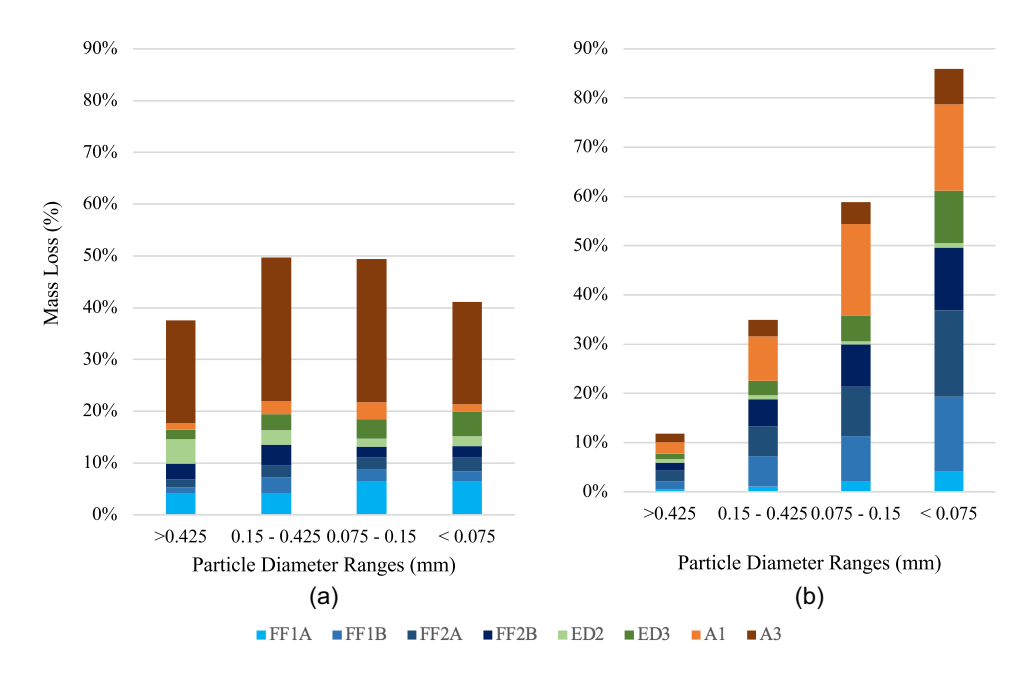


**Fig. 4.** Mass loss in the fractioned ash samples in (a) the 25°C–500°C range; and (b) the 500°C–950°C range. The thickness of each colored bar shows the mass lost during combustion. For Figure 4b, the mass loss in the 25°C–500°C range was subtracted from the LOI value; the figure displays only the mass loss that occurred in the 500°C–950°C range.

**Table 4.** Geotechnical properties of wildfire ashes

	LL	MDW	OMC	Hydraulic conductivity  (×10 <sup>-4</sup> cm/s)				
Sample	(%)	$(kN/m^3)$	(%)	Loose	Dense	Sorptivity $(mm/s^{1/2})$		
FF1A	28.4	16.7	17.5	39.7	1.09	1.70		
FF1B	41.5	13.0	32.8	10.1	1.06	1.84		
FF2A	43.1	14.8	22.1	5.22	0.466	1.17		
FF2B	39.9	15.0	20.4	4.90	0.457	1.59		
ED2	34.7	14.7	19.7	3.86	0.386	1.37		
ED3	38.6	15.7	20.2	2.92	0.158	0.83		
A1	51.8	13.2	29.9	2.46	0.354	1.64		
۸3	82.0	13.3	25.4	a	a	a		

Note: LL = liquid limit; OMC = optimum moisture content; and MDW = maximum dry unit weight.

could not be molded into threads approaching the required 3 mm diameter without cracking.

Sample A3 was an anomaly because it had the highest liquid limit (82.9%) and the highest value of surface area (4.89 m<sup>2</sup>/g) yet the smallest amount of fine-grained material (only 5.8%). Another sample with the same surface area (ED3) and a higher fines content (12%) had an liquid limit (LL) value of 38.6%. Specific surface area is positively correlated with both liquid limit and fines content (Mitchell and Soga 2005), but A3 having little finegrained material indicated that something besides particle diameter was contributing to high liquid limits. A3 was the only sample to have moderate hydrophobicity. Water molecules would not be attracted to the hydrophobic particle surfaces (Doerr et al. 2000), and we hypothesized that additional water was required in the pore spaces and on the hydrophilic surfaces of the ash to generate enough intermolecular cohesion to hold the sample together as a paste which would increase the liquid limit. However, more investigation on how hydrophobicity affects Atterberg limits is needed to explain this phenomenon.

#### Compaction

The maximum dry unit weight of the ashes ranged from 13.0 to  $16.7~\rm kN/m^3$ , with an average value of  $14.6~\rm kN/m^3$  (SD = 1.31) (Table 4). The optimum moisture content ranged from 17.5% to 32.8%, with the lowest OMC corresponding to the burned soil + ash sample (FF1A). The average OMC was 23.5% (SD = 5.4). The compacted void ratios, calculated from weight/volume relationships, were between 0.6 and 1.02.

In Advanced Soil Mechanics, Das (2008) suggested the following typical maximum and minimum values of void ratio and dry unit weights for silty sands: e=0.4–1.0 and  $\gamma_d=13$ –19 kN/m³. The compacted wildfire ashes had lower MDW and higher void ratios than were expected, considering that these samples were compacted to a state of maximum achievable density. Only one sample (FF1A) had a maximum dry unit weight above the average value suggested for silty sands because it was the only sample that was a mixture of burned sand and ash instead of being predominantly ash. The higher void ratios are hypothesized to be due to the unique morphological and chemical characteristics of ash constituents (discussed subsequently).

# **Hydraulic Properties**

The hydraulic conductivity of the pure compacted Silver #20 sand sample was found to be  $9.4 \times 10^{-3}$  cm/s. The equivalent saturated hydraulic conductivity of the two-soil system ranged from  $8.4 \times 10^{-4}$  to  $7.0 \times 10^{-3}$  cm/s for the loose specimens and  $5.9 \times 10^{-5}$ – $3.6 \times 10^{-4}$  cm/s for the dense specimens (Tables 7 and 8). The calculated saturated hydraulic conductivity of the ash layer ranged from  $2.5 \times 10^{-4}$  to  $4.0 \times 10^{-3}$  cm/s for the loose specimens and  $1.6 \times 10^{-5}$ – $1.1 \times 10^{-4}$  cm/s for the dense specimens (Table 4). In general, wildfire ashes had hydraulic conductivity values that were within the expected range for their USCS classification  $(10^{-3}$ – $10^{-5}$  cm/s). However, the authors observed that the ash layers had high void ratios ( $e_{avg} = 1.08$  for dense state and  $e_{avg} = 1.91$  for loose state), even after saturation (Tables 7 and 8). This is likely due to both morphological and chemical characteristics of ash constituents (discussed subsequently).

<sup>&</sup>lt;sup>a</sup>Sample was consumed before measurement could be completed.

Table 5. Friction angles (in degrees) of wildfire ash samples

	Ring	Ring shear				
Sample	Low effective stress range	Entire effective stress range	Dry	Saturated		
FF1A	32.6	29.9	30.7	28.4		
FF1B	41.6	33.9	28.4	27.1		
FF2A	36.5	35.0	30.0	26.1		
FF2B	40.5	33.9	30.1	29.0		
ED2	38.2	32.5	29.2	29.3		
ED3	27.5	33.9	<u></u> a	29.2		
A1	37.0	32.8	29.7	30.3		
A3	25.7	27.7	24.0	a		

<sup>&</sup>lt;sup>a</sup>Sample was consumed before measurement could be completed.

The average sorptivity values for each sample of wildfire ash ranged from 0.83 to 1.84 mm/s<sup>1/2</sup> (Table 4). These values are in the range with other literature on sorptivity of wildfire ashes or wildfire-derived ashes tested using the same device (Balfour and Woods 2013; Moody et al. 2009). The average porosities of specimens ranged from 51% to 72% (average void ratios of 1.05-2.55).

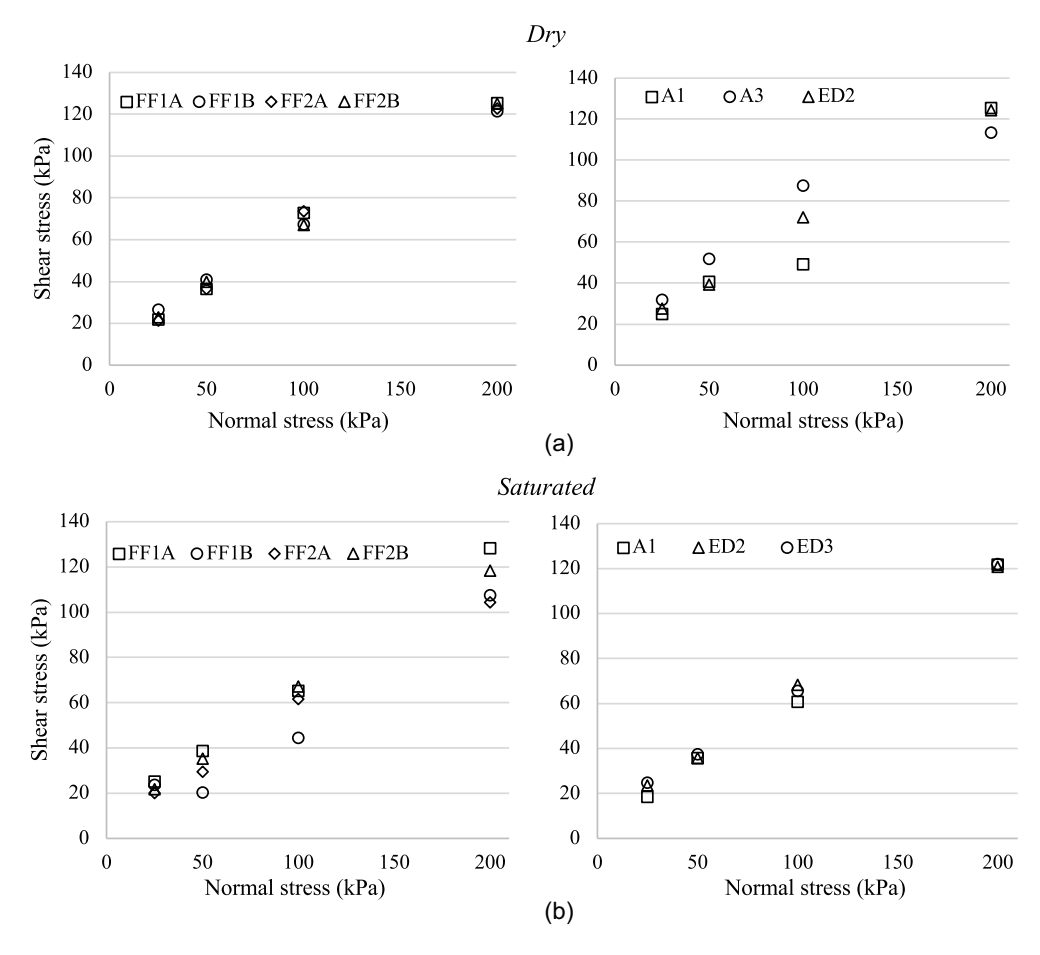
# Strength

The friction angle of the laboratory Silver #20 sand was found to be 40°. The friction angles of the ash/sand layered systems were lower, ranging from 24 to 30.7° (dry condition) and 26–30.3° (saturated

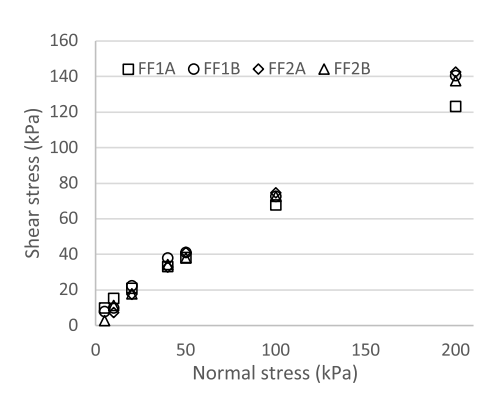
condition) [Table 5; Figs. 5(a and b)]. Cohesion values ranged from 1.2 to 24.7 kPa, but the average cohesion value was 12.5 kPa for all samples tested. Careful observation of samples after shearing confirmed the shearing plane extended through the center of the ash layer. Sample dry unit weights after consolidation (just before shearing) averaged  $13.2 \text{ kN/m}^3$  for the dry condition and  $13.6 \text{ kN/m}^3$  for the saturated condition.

The ring shear friction angle calculated using the entire range of normal stresses (5–200 kPa) ranged from 27.7° to 35° (Table 5; Fig. 6). Cohesion was low, ranging from 2.4 to 10.3 kPa. Thin samples of saturated, fine ash exhibited large displacement friction angles that were higher than those measured using the direct shear device.

An attempt was made using the ring shear device to capture the lowest feasible residual shear strength of the wildfire ashes by running the torsional ring shear tests at very low normal stresses. Samples were prepared at low densities at water contents approaching their liquid limit and only briefly consolidated to 5, 10, 20, and 40 kPa. As soon as the time versus consolidation curve became constant, the shearing was begun. Even under these conditions, samples exhibited friction angles above 25°. In many cases, these samples had higher friction angles that those tested at moderate normal stresses. The cohesion was still low (average c' < 5 kPa). It may be that some wall friction developed due to the intrusion of the top platen into the samples during shearing, which contributed to the variation in the friction angle measured for low and moderate normal stresses (Meehan et al. 2007; Stark and Vettel 1992).



**Fig. 5.** Friction envelopes for direct shear tests showing samples tested in (a) the dry condition; and (b) the saturated condition. Legend abbreviation FF refers to French fire samples, A refers to Apple fire samples, and ED refers to El Dorado fire samples.



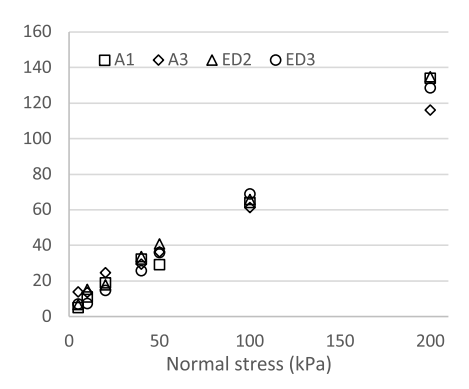


**Fig. 6.** Friction envelopes for ring shear tests using the entire testing range (5–200 kPa). Legend abbreviation FF refers to French fire samples, A refers to Apple fire samples, and ED refers to El Dorado fire samples.

# Relationships between Composition and Geotechnical Behavior

The unique morphologies of wildfire ashes (inorganic minerals such as carbonates with complex surface textures, highly porous, angular, yet soft organic carbon particles, etc.) are a result of a unique formation environment controlled by fuel availability, underlying soils, combustion temperature, and combustion duration (Keeley 2009; Úbeda et al. 2009; and references therein). Others have shown that ash particle sizes, morphologies, color, mineralogy, hydrophobicity, and organic content are related to these conditions (Balfour and Woods 2013; Bodí et al. 2014; DeBano 1981; Pereira et al. 2012; Rodela et al. 2022; Shahack-Gross and Ayalon 2013; Úbeda et al. 2009), and our measurements of wildfire ashes agree with their observations. We suggest that the combustion temperature of our ashes was likely in the range of 300°C–500°C because the ashes contained both coarser organic carbon species and fine carbonate phases.

We hypothesized that the relative percentages of inorganic versus organic constituents in our wildfire ash samples affected how the ashes formed fabrics and so affected their geotechnical properties. To explore this hypothesis, a Pearson correlation coefficient matrix was generated to statistically compare ash geotechnical properties (MDW, OMC, LL, friction angle, etc.) with ash physical and chemical characteristics (% fines, TOC,  $S_s$ , SG, LOI, and TIC) (Table 6).

# Compaction

Although correlation does not imply causation, a consistent strong (r > 0.7) positive correlation between OMC and TIC and OMC and LOI was observed (Table 6). Inversely, a consistent strong negative correlation between MDW and TIC or LOI was also observed. We hypothesized that the carbonate particles in ashes would influence their compaction behavior. Our results showed that ashes with

higher carbonate contents developed fabrics that were looser and more difficult to compact because carbonates had very roughened, complex surface textures, leading to higher interparticle friction between grains, decreasing the MDW and increasing the void ratios of the compacted specimens. Also, because carbonate particles have higher surface areas, more water is required to effectively coat the particles, which would increase the OMC. Balfour and Woods (2013) suggested that the high porosities of carbonate-rich ashes were due to the negative electrostatic charges of carbonates and the formation of a diffuse double layer upon hydration, and this potential effect cannot be discounted. However, additional research is needed to confirm this theory.

# Strength

A negative correlation between TOC and ash friction angle was also observed (Table 6). Increasing the amount of organic content in ash likely weakened the ash matrix. The organic particles in ashes tend to be coarser, more angular, and more heterogeneous than the inorganic fraction (Rodela et al. 2022). We also observed that they crushed easily with slight finger pressure. We believe that these larger, softer particles reduced the contact angles between particles and caused localized softening to develop during shearing, which would decrease the friction angles of ashes with higher organic content (such as the 24° measured for the most organic sample A3). However, the correlation coefficient decreased (r = -0.37) when saturated samples were tested in the direct shear device, possibly because A3 was not tested in the saturated condition. The decrease in the correlation coefficient for the ring shear samples (r = -0.71) may be due to the fact that the ashes tested in the ring shear were sieved over the No. 100 sieve, so the largest organic particles were removed before testing.

In general, the tested wildfire ash samples were relatively stiff, even at low normal stresses and low packing densities. Additionally, the two samples with the highest fines content (A1 and ED2)

Table 6. Pearson correlation coefficients between ash physical and chemical properties and geotechnical properties

Physical and chemical					Geotechn	ical properties			
properties	LL	MDD	OMC	RS FA	Dry DS FA	Saturated DS FA	K, dense	K, loose	Sorptivity
% fine grained	-0.32	-0.39	0.37	0.73	0.48	0.00	-0.72	-0.28	0.22
$S_s (m^2/g)$	0.26	0.35	-0.57	-0.55	-0.54	0.45	0.06	-0.45	-0.65
TOC (%)	0.87	-0.51	0.33	-0.71	-0.98	-0.37	0.01	0.54	0.34
TIC (%)	0.11	-0.74	0.91	0.44	0.05	-0.12	-0.41	0.11	0.40
LOI (%)	0.87	-0.88	0.79	-0.41	-0.83	0.00	-0.39	0.11	0.39

Note: Bolding denotes r values greater than 0.9 (very strong correlations), and italic indicates r values less than 0.7.

also had the highest direct shear friction angles, which is not typical for natural soils, and fine-grained ash specimens tested in the ring shear device had higher friction angles than the direct shear specimens. These observations would indicate that the interparticle friction between the finer ash fraction is high. Because the finer ash particles are composed predominantly of fused nanocrystalline carbonates, once again our results corroborated our hypothesis that the roughened surface textures of these particles created fabrics with higher interparticle friction. The tested samples could maintain high friction angles at low bulk densities.

### Liquid Limit and Other Observations

The organic content and, in the case of sample A3, moderate hydrophobicity of ashes may also have contributed to the higher liquid limit values, based on the correlation coefficient of 0.87 with TOC and LOI. The unburned char particles have a complex internal porosity that may make it more difficult for the particles to become sufficiently hydrated to transition to a liquidy state. However, this may be a case of correlation rather than causation because liquid limit was not correlated with surface area or TIC, when it is well established that surface area is correlated with liquid limit (Mitchell and Soga 2005; Santamarina et al. 2002).

There was no consistent correlation between hydraulic properties and ash composition, but it is worthwhile to mention again that ashes were consistently able to hold a loose fabric structure even when partially or fully saturated. It is uncommon to see naturally occurring silty sands hold void ratios above 1.5 after being fully saturated. We believe the high interparticle friction between particles due to their high surface roughness was responsible for this phenomenon, although, again, influences of electrostatic interactions cannot be discounted.

Hydrophobicity was not shown to affect the geotechnical behavior of wildfire ashes in any case except for the high liquid limit of A3. This is likely due to the fact that the ED2 and FF1A were only slightly water repellent. For testing done in the partially saturated condition (such as sorptivity), the porosity was high enough (ranging from 51% to 72%) that water could easily find preferential flow pathways through the pore openings, even if water did not coat hydrophobic particle surfaces (Doerr et al. 2000). For testing done in the saturated condition (direct shear, ring shear, and hydraulic conductivity), enough water and sufficient time were given before testing to overcome any initial wetting boundary provided by the slightly hydrophobic nature of the ash, and as the water content approaches saturation, water repellency effects were severely diminished (Doerr et al. 2000). Unfortunately, sample A3 was consumed before sorptivity and hydraulic conductivity could be measured, so the effect of moderate water repellency could not be analyzed. It is likely that geotechnical properties of partially saturated soils would be affected by moderate to severe water repellency; testing of hydrophobic ashes should be done to examine this effect on behavior.

We have identified the following research gaps to be addressed:

- 1. Additional strength testing of wildfire ash using a static and cyclic triaxial device should be performed. A triaxial testing device would allow the researcher to measure both the undrained and drained strength of the material, and dynamic triaxial testing would provide more insight into how ashes may potential liquefy at high water contents. Unfortunately, due to COVID-19, triaxial equipment was unavailable to the research team at the time of publication. This additional testing would provide more information about the potential stability of carbonate-rich wildfire ashes in situ.
- 2. Electrostatic bonding between mineral phases may also contribute to ash low bulk density and high void ratios. The electrostatic

- potential of wildfire ashes and the formation of a carbonate diffuse double layer that would affect fabric formation should be investigated, particularly for ashes combusted at temperatures above 350°C (Balfour and Woods 2013).
- 3. The suite of tests summarized in this manuscript should be run on more ashes from additional wildfire sites, so that a larger database of ash index and geotechnical properties can be developed. Particular attention should be focused on testing hydrophobic and highly organic ashes.
- 4. In general, it would be helpful if ash sampling methods and chemical analysis methods were standardized across wildfire ash studies, as suggested by Sánchez-García et al. (2023), so that characteristics reported by others could more easily be compared across studies.

#### **Conclusions**

Wildfire ashes from three different fire sites in California were characterized using a variety of physical (grain size distribution, SG, SSA, etc.), chemical (LOI, carbon isotopes, elemental composition, etc.), and standard geotechnical engineering (compaction, hydraulic conductivity, Atterberg limits, and shear strength) methods. Ashes were composed of organic char and inorganic mineral ash (predominantly carbonates) derived from the combustion of plant biomass. Chemical analysis of the ashes showed that the inorganic constituents were predominantly silica, aluminum, and calcium, but the organic versus inorganic fraction varied from wildfire site to wildfire site and between samples taken at the same site. Index testing confirmed that although wildfire ashes had particles sizes and specific gravities in the range for silty sands, they had unusually high specific surface areas. The specific surface areas were high because the carbonate and char morphologies present in the ash had highly texturized and porous surfaces, respectively. We anticipate that, due to the abundance of carbonate species in the ashes tested, the combustion temperatures of these samples were in the realm of 300°C–500°C.

We hypothesized that the unique morphologies in our wildfire ashes directly influenced their geotechnical behavior, and our results demonstrated that mineral phases with roughed surface textures affected specimen geotechnical properties such as strength, liquid limit, sorptivity, and density. Specimens had high sorptivity, medium permeability, and friction angles ranging from 24° to 30.7°. Additionally, high void ratios and low bulk densities were consistently observed during geotechnical testing. Specimen liquid limits approaching and exceeding 40% and high optimum moisture contents would indicate that the tested ashes had morphologies with complex surface textures that required much water to hydrate effectively. The low maximum dry density, consistently high void ratios, high sorptivity, and high friction angles, even when specimens were partially or fully saturated, were attributed to the ash loose fabric structure. The loose fabric structure was attributed to ash mineral phases with roughened surface morphologies, such as the fused nanocrystalline calcium carbonate phases. In general, because the formation of specific components in ash is related to fuel availability and combustion environment and the macroscale geotechnical properties of ash are influenced by these microscale components, we propose that the geotechnical behavior of ashes depends on ash formation environment.

# Appendix. Supplementary Information

Tables 7 and 8 contain additional quantitative information about the saturated hydraulic conductivity of wildfire ash specimens that

**Table 7.** Hydraulic conductivity of dense specimens (relative compaction 85%)

Sample	Void ratio	$k_{\rm eq,system}$ (cm/s)	$k_{\rm ash}~({\rm cm/s})$
FF1A	0.67	$3.63 \times 10^{-4}$	$1.09 \times 10^{-4}$
FF1B	1.47	$3.03 \times 10^{-4}$	$1.06 \times 10^{-4}$
FF2A	1.06	$1.25 \times 10^{-4}$	$4.66 \times 10^{-5}$
FF2B	1.02	$1.24 \times 10^{-4}$	$4.57 \times 10^{-5}$
ED2	1.05	$1.19 \times 10^{-4}$	$3.86 \times 10^{-5}$
ED3	0.95	$5.88 \times 10^{-5}$	$1.58 \times 10^{-5}$
A1	1.32	$1.12 \times 10^{-4}$	$3.54 \times 10^{-5}$

**Table 8.** Hydraulic conductivity of loose specimens (relative compaction 50%)

Sample	Void ratio	$k_{\rm eq,system}$ (cm/s)	$k_{\rm ash}~({\rm cm/s})$
FF1A	1.28	$7.01 \times 10^{-3}$	$3.97 \times 10^{-3}$
FF1B	2.70	$2.28 \times 10^{-3}$	$1.01 \times 10^{-3}$
FF2A	2.01	$1.41 \times 10^{-3}$	$5.22 \times 10^{-4}$
FF2B	1.61	$1.44 \times 10^{-3}$	$4.90 \times 10^{-4}$
ED2	2.01	$1.20 \times 10^{-3}$	$3.12 \times 10^{-4}$
ED3	1.51	$1.22 \times 10^{-3}$	$2.92 \times 10^{-4}$
A1	2.27	$8.35 \times 10^{-4}$	$2.46 \times 10^{-4}$

were prepared as a thick layer above a layer of laboratory Silver #20 sand. The void ratios of the ash layers after saturation are also reported.

# **Data Availability Statement**

Some or all data, models, or code generated or used during the study are available in the NHERI DesignSafe repository in accordance with funder data retention policies [(2023) *Characterization and Geotechnical Properties of Wildfire Ashes*. DesignSafe-CI., DOIs: 10.17603/ds2-5g4s-0d41; 10.17603/ds2-z44q-yx40; 10.17603/ds2-02jz-3v08; 10.17603/ds2-kkzm-6056; 10.17603/ds2-t4qr-g268; 10.17603/ds2-d4n9-kk33; 10.17603/ds2-bs6z-4258; 10.17603/ds2-e0tv-4q57; 10.17603/ds2-5c1g-jq39; 10.17603/ds2-r93e-7d76; 10.17603/ds2-54es-sq16; 10.17603/ds2-jfjy-0122]. A portion of this work is a published part of the conference proceedings for the 9th International Congress on Environmental Geotechnics (Wirth et al. 2023).

# **Acknowledgments**

This work was funded in part by NSF Award #2138449. We graciously acknowledge the support provided by the National Science Foundation. We would like to acknowledge the efforts of former research students John Navarette and Brayden Padilla, whose contributions were instrumental in developing this work. Additionally, we would like to thank Dr. Matthew Kirby and Dr. Sean Loyd of the Geological Sciences department at CSU Fullerton, without whose guidance and equipment the particle size analysis and carbonate/carbon isotope testing would not have been possible. We would also like to thank Nick Everett Rollins and Dr. William Berelson of the University of Southern California for the use of the SEM. Finally, we would like to thank Boral Resources for the use of their helium pycnometer and X-ray fluorescence equipment. This work would not have been completed without the assistance of these individuals.

#### References

- Araújo Santos, L., S. Lopes, and J. Silva. 2019. "Difficulties of using the Harvard miniature compaction apparatus as a reference test in the study of soil compaction." In Proc., 17th European Conference on Soil Mechanics and Geotechnical Engineering. Lisbon, Portugal: Portuguese Geotechnical Society.
- Araújo Santos, L. M., A. J. P. M. Correia, and P. A. L. F. Coelho. 2020. "Post-wildfire slope stability effects and mitigation: A case study from hilly terrains with unmanaged forest." *SN Appl. Sci.* 2 (11): 1–21. https://doi.org/10.32075/17ECSMGE-2019-0620.
- ASTM. 2000. Standard test method for permeability of granular soils (constant head). ASTM D2434. West Conshohocken, PA: ASTM.
- ASTM. 2010. Standard test methods for liquid limit, plastic limit, and plasticity index of soils. ASTM D4318. West Conshohocken, PA: ASTM.
- Balfour, V. N., and S. W. Woods. 2013. "The hydrological properties and the effects of hydration on vegetative ash from the northern Rockies, USA." *Catena* 111 (Dec): 9–24. https://doi.org/10.1016/j.catena.2013 .06.014.
- Bodí, M. B., D. A. Martin, V. N. Balfour, C. Santín, S. H. Doerr, P. Pereira, A. Cerdà, and J. Mataix-Solera. 2014. "Wildland fire ash: Production, composition and eco-hydro-geomorphic effects." *Earth Sci. Rev.* 130 (Mar): 103–127. https://doi.org/10.1016/j.earscirev.2013.12.007.
- Bodí, M. B., J. Mataix-Solera, S. H. Doerr, and A. Cerdà. 2011. "The wettability of ash from burned vegetation and its relationship to Mediterranean plant species type, burn severity and total organic carbon content." *Geoderma* 160 (3–4): 599–607. https://doi.org/10.1016/j.geoderma.2010.11.009.
- Budhu, M. 2011. Soil mechanics and foundations. Hoboken, NJ: Wiley. Cannon, S. H., and J. Degraff. 2015. "Cascading consequences of climate change and expanding population on the threat of wildfire and post fire debris-flow hazards, Western U.S." In Landslides: Disaster risk reduction, 177–190. Berlin: Springer-Verlag.
- Cannon, S. H., J. E. Gartner, A. Holland-Sears, B. M. Thurston, and J. A.
  Gleason. 2003. "Debris flow response of basins burned by the 2002
  Coal Seam and Missionary Ridge fires, Colorado." In Engineering geology in Colorado: Contributions, tends, and case histories, 1–31.
  Golden, CO: Colorado Geological Survey.
- Cerdà, A., and S. H. Doerr. 2008. "The effect of ash and needle cover on surface runoff and erosion in the immediate post-fire period." *Catena* 74 (3): 256–263. https://doi.org/10.1016/j.catena.2008.03.010.
- Certini, G. 2005. "Effects of fire on properties of forest soils: A review."

  Oecologia 143 (1): 1–10. https://doi.org/10.1007/s00442-004-1788-8.
- Das, B. M. 2008. Advanced soil mechanics. New York: Taylor & Francis.
   Debano, L. F. 1999. "Fire-induced water repellency in soils: Hydrologic implications." Hydrol. Water Resour. Arizona Southwest 29: 1–7.
- DeBano, L. F. 1981. Water repellent soils: A state-of-the-art. Berkeley, CA: Pacific Southwest Forest and Range Experiment Station.
- De Graff, J. V. 2018. "A rationale for effective post-fire debris flow mitigation within forested terrain." *Geoenviron. Disasters* 5 (7): 1–9. https://doi.org/10.1186/s40677-018-0099-z.
- Doerr, S. H., R. A. Shakesby, and R. P. D. Walsh. 2000. "Soil water repellency: Its causes, characteristics and hydro-geomorphological significance." *Earth Sci. Rev.* 51 (1–4): 33–65. https://doi.org/10.1016/S0012-8252(00)00011-8.
- Ebel, B. A., J. A. Moody, and D. A. Martin. 2012. "Hydrologic conditions controlling runoff generation immediately after wildfire." *Water Resour. Res.* 48 (3): 1–13. https://doi.org/10.1029/2011WR011470.
- Keeley, J. 2009. "Fire intensity, fire severity and burn severity: A brief review and suggested usage." *Int. J. Wildland Fire* 18 (1): 116–126. https://doi.org/10.1071/WF07049.
- Kohn, M. J. 2010. "Carbon isotope compositions of terrestrial C3 plants as indicators of (paleo)ecology and (paleo)climate." *Proc. Natl. Acad. Sci.* U.S.A. 107 (46): 19691–19695. https://doi.org/10.1073/pnas.1004933107.
- Lambe, T. W., and R. V. Whitman. 1969. Soil mechanics. Chichester, UK: Wiley.
- Larsen, I. J., L. H. MacDonald, E. Brown, D. Rough, M. J. Welsh, J. H. Pietraszek, Z. Libohova, J. Dios Benavides-Solorio, and K. Schaffrath. 2009. "Causes of post-fire runoff and erosion: Water repellency, cover,

- or soil sealing?" Soil Sci. Soc. Am. J. 73 (4): 1393–1407. https://doi.org/10.2136/sssaj2007.0432.
- Meehan, C. L., T. L. Brandon, and J. M. Duncan. 2007. "Measuring drained residual strengths in the bromhead ring shear." *Geotech. Test. J.* 30 (6): 466–473. https://doi.org/10.1520/GTJ101017.
- Mitchell, J. K., and K. Soga. 2005. "Chapter 04." Fundam. Soil Behhav. (3): 83–108.
- Monje, P. V., and E. J. Baran. 2002. "Characterization of calcium oxalates generated as biominerals in cacti." *Plant Physiol*. 128 (2): 707–713. https://doi.org/10.1104/pp.010630.
- Moody, J. A., B. A. Ebel, P. Nyman, D. A. Martin, C. Stoof, and R. Mckinley. 2016. "Relations between soil hydraulic properties and burn severity." *Int. J. Wildland Fire* 25 (3): 279–293. https://doi.org/10 .1071/WF14062.
- Moody, J. A., D. A. Kinner, and X. Úbeda. 2009. "Linking hydraulic properties of fire-affected soils to infiltration and water repellency." *J. Hydrol.* 379 (3–4): 291–303. https://doi.org/10.1016/j.jhydrol.2009 .10.015.
- Moody, J. A., R. A. Shakesby, P. R. Robichaud, S. H. Cannon, and D. A. Martin. 2013. "Current research issues related to post-wildfire runoff and erosion processes." *Earth Sci. Rev.* 122 (Jul): 10–37. https://doi.org/10.1016/j.earscirev.2013.03.004.
- Neary, D. G., G. J. Gottfried, and P. F. Ffolliott. 2003. "Post-wildfire watershed flood responses." In Proc., 2nd Int. Fire Ecology and Fire Management Congress, 1–8. Boston: American Meteorological Society.
- Onda, Y., W. E. Dietrich, and F. Booker. 2008. "Evolution of overland flow after a severe forest fire, Point Reyes, California." *Catena* 72 (1): 13–20. https://doi.org/10.1016/j.catena.2007.02.003.
- Parker, V., R. Pratt, and J. E. Keeley. 2018. "Chaparral." Encycl. Ecol. 420–425.
- Pereira, P., A. Cerdà, X. Úbeda, J. Mataix-Solera, D. Martin, A. Jordán, and M. Burguet. 2013. "Spatial models for monitoring the spatio-temporal evolution of ashes after fire—A case study of a burnt grassland in Lithuania." Solid Earth 4 (1): 153–165. https://doi.org/10.5194/se-4 -153-2013.
- Pereira, P., X. Úbeda, and D. A. Martin. 2012. "Fire severity effects on ash chemical composition and water-extractable elements." Geoderma 191 (Dec): 105–114. https://doi.org/10.1016/j.geoderma .2012.02.005.
- Rodela, M. H., I. Chowdhury, and A. K. Hohner. 2022. "Emerging investigator series: Physicochemical properties of wildfire ash and implications for particle stability in surface waters." *Environ. Sci. Process. Impacts* 24 (11): 2129–2139. https://doi.org/10.1039 /D2EM00216G.

- Sánchez-García, C., et al. 2023. "Chemical characteristics of wildfire ash across the globe and their environmental and socio-economic implications." *Environ. Int.* 178 (Aug): 108065. https://doi.org/10.1016/j .envint.2023.108065.
- Santamarina, J. C., K. A. Klein, and M. A. Fam. 2001. Soils and waves. Chichester, UK: Wiley.
- Santamarina, J. C., K. A. Klein, Y. H. Wang, and E. Prencke. 2002. "Specific surface: Determination and relevance." *Can. Geotech. J.* 39 (1): 233–241. https://doi.org/10.1139/t01-077.
- Shahack-Gross, R., and A. Ayalon. 2013. "Stable carbon and oxygen isotopic compositions of wood ash: An experimental study with archaeological implications." *J. Archaeolog. Sci.* 40 (1): 570–578. https://doi.org/10.1016/j.jas.2012.06.036.
- Stark, T. D., and J. Vettel. 1992. "Bromhead ring shear test procedure." Geotech. Test. J. 15 (1): 24–32. https://doi.org/10.1520/GTJ10221J.
- Tiwari, B., B. Ajmera, A. Gonzalez, and H. Sonbol. 2020. "Impact of wild-fire on triggering mudslides: A case study of 2018 Montecitro debris flows." In *Proc.*, *Geo-Congress* 2020 Conf., 289–298. Reston, VA: ASCE.
- Úbeda, X., P. Pereira, L. Outeiro, and D. A. Martin. 2009. "Effects of fire temperature on the physical and chemical characteristics of the ash from two plots of cork oak (*Quercus suber*)." *Land Degrad. Dev.* 20 (6): 589–608. https://doi.org/10.1002/ldr.930.
- Vassilev, S. V., D. Baxter, and C. G. Vassileva. 2013. "An overview of the behaviour of biomass during combustion: Part I. Phase-mineral transformations of organic and inorganic matter." Fuel 112 (Oct): 391–449. https://doi.org/10.1016/j.fuel.2013.05.043.
- Wirth, X., V. Antunez, D. Enriquez, and Z. Arevalo. 2023. "Engineering properties of wildfire ashes." In *Proc.*, 9th Int. Congress on Environmental Geotechnics, 1–10. London: International Society for Soil Mechanics and Geotechnical Engineering.
- Wirth, X., D. A. Glatstein, and S. E. Burns. 2019. "Mineral phases and carbon content in weathered fly ashes." Fuel 236 (Jan): 1567–1576. https://doi.org/10.1016/j.fuel.2018.09.106.
- Woods, S. W., and V. N. Balfour. 2010. "The effects of soil texture and ash thickness on the post-fire hydrological response from ash-covered soils." J. Hydrol. 393 (3–4): 274–286. https://doi.org/10.1016/j .jhydrol.2010.08.025.
- Yeboah, N. N. N., C. R. Shearer, S. E. Burns, and K. E. Kurtis. 2014. "Characterization of biomass and high carbon content coal ash for productive reuse applications." *Fuel* 116 (Jan): 438–447. https://doi.org/10.1016/j.fuel.2013.08.030.
- Zhang, R. 1997. "Infiltration models for the disk infiltrometer." *Soil Sci. Soc. Am. J.* 61 (6): 1597–1603. https://doi.org/10.2136/sssaj1997.03615995006100060008x.